PROCEEDINGS OF SCIENCE

Multiple shock acceleration in active galactic nucleus jets

Ana Laura Müller[a,*] **and Anabella Araudo**[a,b]

[a] *Extreme Light Infrastructure ERIC,ELI Beamlines Facility, Za Radnicí 835, CZ-25241 Dolní Břežany, Czech Republic*

[b] *Laboratoire Univers et Particules de Montpellier (LUPM) Université Montpellier, CNRS/IN2P3, CC72, place Eugène Bataillon, 34095, Montpellier Cedex 5, France*

E-mail: analaura.muller@eli-beams.eu, anabella.araudo@eli-beams.eu

Radiogalaxies are the subclass of active galactic nuclei where large-scale relativistic jets are detected. In this work we study the acceleration of particles in a multiple shock scenario produced by the collision of the relativistic jets with embedded massive stars. We solve the transport equation taking into account not only the spatial and radiative losses but also the collective effect of the shocks and the possible reacceleration, and evaluate the maximum energies that the particles can achieve. Finally, we compute the gamma-ray emission expected in this scenario and discuss the detection possibilities.

7th Heidelberg International Symposium on High-Energy Gamma-Ray Astronomy (Gamma2022)
4-8 July 2022
Barcelona, Spain

*Speaker

PoS(Gamma2022)077

1. INTRODUCTION

Active galactic nuclei (AGNs) with misaligned jets are gamma-ray emitters observed at GeV and TeV energies. Nevertheless, their emission mechanism remains unknown. In [1–3], the authors considered that the interaction of AGN jets with massive stellar winds is a suitable scenario for TeV particle acceleration and gamma-ray emission. We note however that if several stars are simultaneously inside the jet, particles can be reaccelerated at multiple shocks. In the present contribution we explore this possibility.

The collision of the AGN relativistic jet with the wind of an ambient star leads to the production of a pair of shocks. The shock in the wind is non-relativistic with velocity $v_{\rm sh,w} \sim v_\infty$, where v_∞ is the terminal wind speed. On the other hand, the shock in the jet is relativistic with a velocity $v_{\rm sh,j} \sim v_{\rm jet}$. The stagnation point of the bowshock around the stars can be found by matching the jet and wind ram pressures [4]. For a jet with kinetic luminosity $L_{\rm jet}$ and a wind with mass loss rate $\dot{M}_\star$ we find that the stagnation point locates at a distance

$$R_{\rm sp}(z) = \sqrt{\frac{\dot{M}_\star\, v_\infty\, v_{\rm jet}\, R^2_{\rm jet}(z)}{4\, L_{\rm jet}}} \propto z \tag{1}$$

from the star, where $R_{\rm jet}(z) = z\,\tan(\theta)$ with θ the opening angle of the jet and z the height in the jet (see Fig. 1).

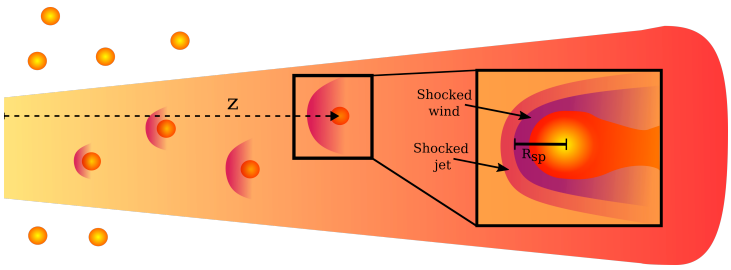

Figure 1: Sketch of our scenario. The interaction of each star with the jet produces a pair of shocks. The distance between the centre of the star and the contact discontinuity increases with the height z, as indicated in Eq. 1.

2. MODEL

For our first analysis, we concentrate only on electron acceleration. We consider the jet encountering massive stars since their strong winds create a favourable environment to produce significant radiation by the interaction of relativistic electrons with the magnetic and photon fields. On the other hand, the emission generated by relativistic protons becomes negligible because of the low particle density at $R_{\rm sp}$. Jet-massive star interactions have also been likely related to the stationary X-ray knots observed in Centaurus A [5, 6]. As sketched in Fig. 1, the interactions lead to the formation of several bowshocks along the jet. This situation is very promising for multiple-shock acceleration.

We calculate the electron distributions taking into account the particle injection at the bowshocks, the propagation effects between shocks, the reacceleration, and the energy losses. We proceed as follows

1. First, we assume that particles are accelerated in the shock into the wind, which is non-relativistic, by diffusive shock acceleration [7, 8]. Since we focus on interactions with massive young stars whose typical wind velocities are thousands of km s^{-1}, we assume a Fermi I injection $S(p) = S_0 p^{-\alpha}\, e^{-p/p_{\rm max}}$ with $\alpha = 4$, and the maximum momentum $p_{\rm max}$ determined by equating the acceleration and losses timescales. The normalization S_0 is calculated from the kinetic power of the wind as in [3]. We solve the stationary kinetic equation to find the particle distribution $f(p)$. The radiative losses considered are synchrotron, ionization, relativistic Bremsstrahlung, inverse Compton (IC) with the photons of the star and the Cosmic Microwave Background (CMB), and synchrotron self-Compton, whereas the escape includes the diffusion and convection of the particles out of the acceleration region. Expressions for these losses can be found in, e.g., [3] and references therein.

2. Once the particles escape the shock in the stellar wind, they are carried along the jet convected with the outflow material. We propagate the particle distribution $f(p)$ obtained in the previous step to the next bowshock position. During propagation, we do not consider any acceleration, only radiative and escape losses. We introduce the fraction $(R_{\rm sp}(z)/R_{\rm jet}(z))^2$ to account for the fact that not all the particles injected by a shock will encounter the next one. To obtain the particle distribution reaching the following shock $f_{\rm prop}(p)$, we solve the transport equation with temporal and momentum dependency.

3. Once electrons reach a new bowshock, they are reaccelerated in the mildly relativistic shock in jet. For calculating the reaccelerated particle distribution, we use the following expression [see e.g., 9–11]

$$f_{\rm reacc}(p) = \alpha_{\rm rel} \int_{p_0}^{p} \frac{dp'}{p'}\, f_{\rm prop}(p') \left(\frac{p}{p'}\right)^{-\alpha_{\rm rel}} \tag{2}$$

   with $\alpha_{\rm rel} = 4.3$. In Eq. (2), the background particle distribution is the one obtained after propagation. Equation 2 is formally derived for the case of non-relativistic shocks. Nevertheless, since $\Gamma = 5$, our shocks are mildly relativistic and therefore we adopt Eq. (2) for our preliminary calculations. The maximum energy of the particles is set by the timescales of the losses and applied to the reaccelerated distribution as an exponential cut-off.

4. We repeat all the previous steps in a loop according to the number of shocks.

3. PRELIMINARY RESULTS

We adopt the characteristic values $v_\infty = 3000\,{\rm km\ s^{-1}}$ and $\dot{M}_\star = 10^{-4}\,{\rm M_\odot\ yr^{-1}}$. For the stellar surface temperature and luminosity we assume $T_\star = 3 \times 10^4\,{\rm K}$ and $L_\star = 10^{39}\,{\rm erg\,s^{-1}}$, respectively. In the case of the AGN jet, we assume $L_{\rm jet} = 10^{43}\,{\rm erg\,s^{-1}}$, a macroscopic Lorentz factor $\Gamma = 5$, and opening angle $\theta = 5^\circ$ [3]. The mass of the AGN black hole adopted is $10^8\ {\rm M_\odot}$. The magnetic field of the jet is assumed to evolve with the distance z as $B_{\rm jet}(z) = B_0(z_0/z)$, where B_0 and z_0 are defined by requiring equipartition between the magnetic and kinetic energy ($L_{\rm jet}$) of the jet at the position of the jet basis [see e.g., 12, 13]. For the star magnetic field, we use the expressions given by [14].

3.1 Maximum energies and particle distributions

With the set of parameters specified above, the convection of particles dominates the losses in the stellar wind and the jet along almost the whole energy range. Nevertheless, Fig. 2 shows that the maximum electron energies in the shocks are determined by the synchrotron losses. Matching the acceleration and synchrotron timescales we found that the maximum energy for the particles in a shock in the jet at z is $E^e_{\rm max,jet} \propto \sqrt{B^{-1}_{\rm jet}(z)} \propto \sqrt{z}$, i.e., at larger distances it is possible to accelerate electrons up to slightly larger energies. Figure 2 also indicates that relativistic Bremsstrahlung becomes negligible and gamma rays can be produced by IC scattering, however this emission is expected to be several orders of magnitude smaller than the synchrotron luminosity.

Electrons accelerated in the wind shocks achieve a maximum energy $E^e_{\rm max,w} = 13$ TeV, whereas the reacceleration can boost the particles up to 1.3 PeV. According to the star distributions used by [3], thousands of massive stars should exist inside the first kpc of the jet. Since we are focused on the case of bright stars with the most powerful winds, only a small number of those stars should be well represented by the adopted star parameters. Therefore, we study the conservative case of ten massive stars arbitrarily distributed within 200 and 600 pc. The left panel in Fig. 3 compares the particle distribution for two consecutive shocks using the approach described in Section 2. Losses during propagation between two consecutive shocks are also dominated by synchrotron, and therefore particles arrive to the next shock with a smaller energy. The reacceleration generates a tail of particles above the cut-off energy of the wind shock. This hump of particles could produce distinctive features in the spectral energy distribution (SED) of jetted AGN. The total particle distributions for four of the ten shocks are displayed in the right panel in Fig. 3.

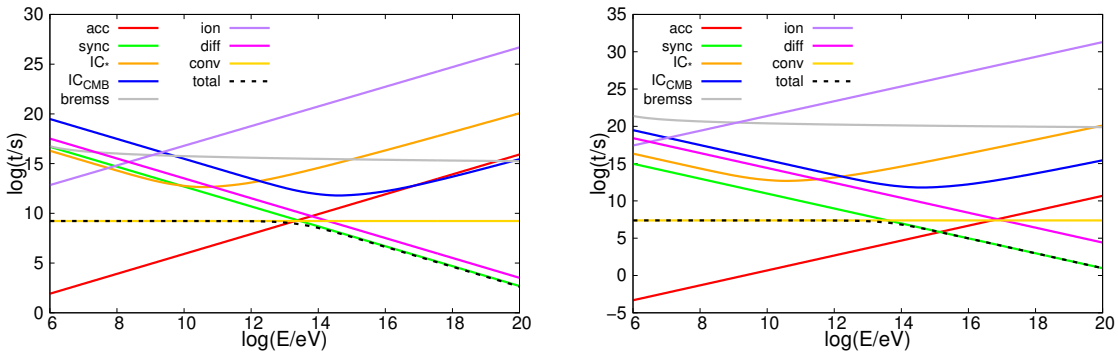

Figure 2: Acceleration, escape, and cooling timescales at the shock into the wind (left) and jet (right).

3.2 Non-thermal emission

We compute the SED for all the relevant radiative processes. Expressions for these calculation can also be found in, e.g., [3]. Figure 4 shows that the reaccelerated particles produce a hump in the spectrum between the X-ray and gamma-ray bands, changing the shape predicted in works without reacceleration. Nevertheless, the SED indicates that the individual detection at the higher energies is not possible and that the integrated emission detection requires a large amount of massive stars inside the jet. Therefore, a more detailed characterisation of the stellar population close to the AGN jet is required in order to clarify the feasibility of observing the emission from these systems.

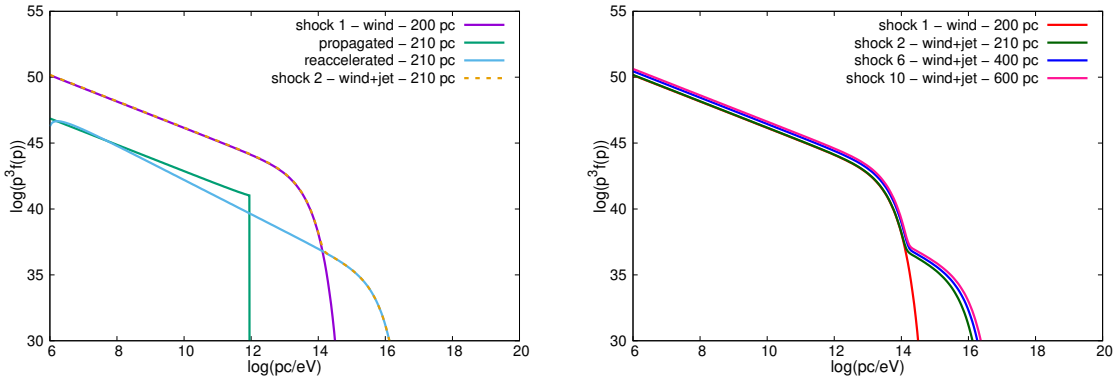

Figure 3: Left: particle distribution injected by the shock into the wind at the first bowshock (solid purple line), distribution encountering the second bowshock after propagation (solid green line), particle distribution resulting from reacceleration (solid light-blue line), and total particle distribution at the second bowshock (dashed orange line). Right: electron distribution at different bowshock distances.

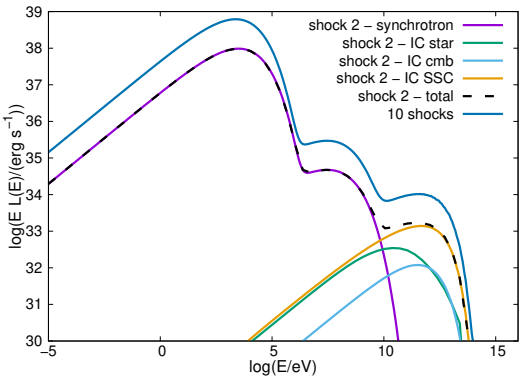

Figure 4: Spectral energy distribution. The purple, orange, green, and light blue solid lines are the synchrotron, synchrotron self-Compton, IC with photons of the star, and IC with photons of the CMB, respectively. The dashed black line is the total emission expected from one bowshock, whereas the solid dark-blue line is the integrated emission from the 10 bowshocks.

4. CONCLUSIONS

The interaction of massive stars with AGN jets is a promising scenario for particle acceleration and non-thermal emission. In this work we present our preliminary results for the reacceleration of electrons in multiple shocks. Electrons are injected through Fermi I acceleration mechanism in each bowshock and reaccelerated by the shocks at larger z. We find that the spectrum of reaccelerated particles extends up to larger energies and becomes flatter after multiple interactions, as expected. We also find a characteristic bump in the SED between 10^5 and 10^{10} eV which does not appear in previous studies without reacceleration. Nevertheless, observing the new spectral features depends on the number of massive stars inside the jet and more accurate predictions require a better characterisation of the stellar population close to the AGN jet.

Acknowledgments

The authors thank the Czech Science Foundation under the grant GAČR 20-19854S. A.T.A thanks the Marie Skłodowska-Curie fellowship.

References

[1] W. Bednarek and R.J. Protheroe, *Testing the homogeneous synchrotron self-Compton model for gamma-ray production in Mrk421*, *Mon. Not. R. Astron. Soc.* **292** (1997) 646.

[2] M.V. Barkov, F.A. Aharonian and V. Bosch-Ramon, *Gamma-ray Flares from Red Giant/Jet Interactions in Active Galactic Nuclei*, *Astrophys. J.* **724** (2010) 1517 [1005.5252].

[3] A.T. Araudo, V. Bosch-Ramon and G.E. Romero, *Gamma-ray emission from massive stars interacting with active galactic nuclei jets*, *Mon. Not. R. Astron. Soc.* **436** (2013) 3626 [1309.7114].

[4] W. Bednarek and R.J. Protheroe, *Gamma-rays from interactions of stars with active galactic nucleus jets*, *Mon. Not. R. Astron. Soc.* **287** (1997) L9 [astro-ph/9612073].

[5] S. Wykes, M.J. Hardcastle, A.I. Karakas and J.S. Vink, *Internal entrainment and the origin of jet-related broad-band emission in Centaurus A*, *Mon. Not. R. Astron. Soc.* **447** (2015) 1001 [1409.5785].

[6] B. Snios, P.E.J. Nulsen, R.P. Kraft, C.C. Cheung, E.T. Meyer, W.R. Forman et al., *Detection of Superluminal Motion in the X-Ray Jet of M87*, *Astrophys. J.* **879** (2019) 8 [1905.04330].

[7] A.R. Bell, *The acceleration of cosmic rays in shock fronts - I.*, *Mon. Not. R. Astron. Soc.* **182** (1978) 147.

[8] R.D. Blandford and J.P. Ostriker, *Particle acceleration by astrophysical shocks.*, *Astrophys. J. Lett.* **221** (1978) L29.

[9] R.D. Blandford and J.P. Ostriker, *Supernova shock acceleration of cosmic rays in the Galaxy.*, *Astrophys. J.* **237** (1980) 793.

[10] P. Schneider, *Diffusive particle acceleration by an ensemble of shock waves*, *Astron. Astrophys.* **278** (1993) 315.

[11] M. Cardillo, E. Amato and P. Blasi, *Supernova remnant W44: a case of cosmic-ray reacceleration*, *Astron. Astrophys.* **595** (2016) A58 [1604.02321].

[12] J.H. Krolik, *Active galactic nuclei : from the central black hole to the galactic environment*, Princeton University Press (1999).

[13] G.E. Romero, M. Boettcher, S. Markoff and F. Tavecchio, *Relativistic Jets in Active Galactic Nuclei and Microquasars*, *Space Sci. Rev.* **207** (2017) 5 [1611.09507].

[14] D. Eichler and V. Usov, *Particle Acceleration and Nonthermal Radio Emission in Binaries of Early-Type Stars*, *Astrophys. J.* **402** (1993) 271.